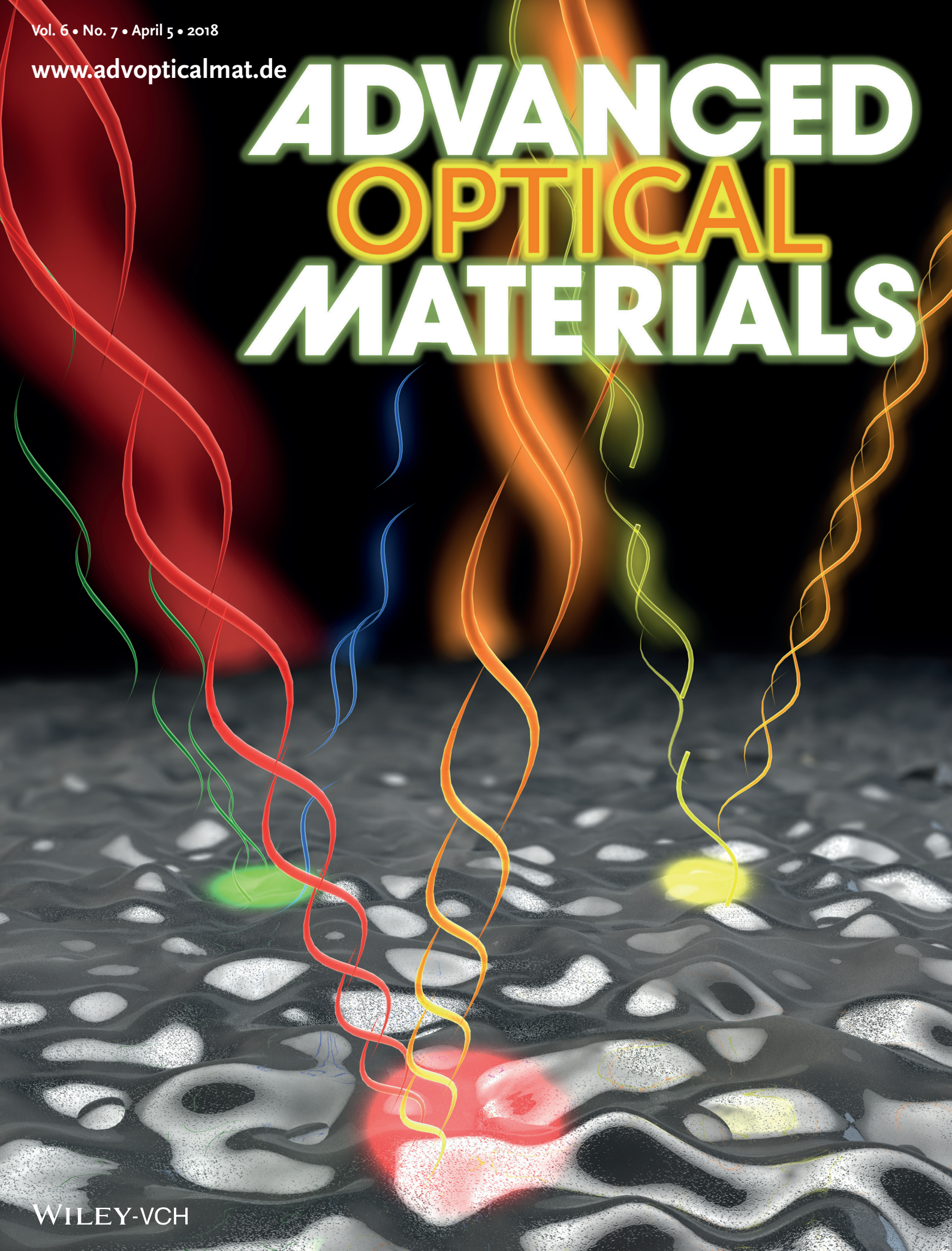


Vol. 6 • No. 7 • April 5 • 2018

www.advopticalmat.de

ADVANCED OPTICAL MATERIALS



WILEY-VCH

Active Control of Photon Recycling for Tunable Optoelectronic Materials

Yunlu Xu, Elizabeth M. Tennyson, Jehyung Kim, Sabyasachi Barik, Joseph Murray, Edo Waks, Marina S. Leite, and Jeremy N. Munday*

Optoelectronic materials are the backbone of today's high-tech industry. To customize their response, one can directly modify the atomic arrangement, chemical composition, lattice strain, or doping of the semiconductor. However, these processes frequently cause undesirable effects resulting from induced defects. Here, a novel concept is demonstrated to actively tune the optoelectronic response of a material through tailored photon recycling. Without altering the material's intrinsic structure, doping, or temperature, the reabsorption of emitted photons within GaAs is modulated to control its carrier density. This approach is used to create a diode that can change its emission wavelength, a solar cell with improved open-circuit voltage, and an actively controlled, gate-free current modulator. These results represent a new platform to enable materials with tailored optoelectronic response based on photonic manipulation rather than semiconductor engineering.

The ability to engineer both the optical and electrical responses of semiconductors has revolutionized the optoelectronics industry^[1–7]—encompassing the development of semiconductor lasers, multijunction solar cells, light emitting diodes (LEDs), and photodetectors. The performance of these devices heavily depends on the bandgap of their active layers, which is an intrinsic property of the material.^[8] The ability to control light absorption and emission by tuning the semiconductor bandgap has made possible lasers based on III-V heterostructures,^[9,10]

high-efficiency, strain engineered multi-junction solar cells,^[11] and blue LEDs.^[12] Nevertheless, these existing pathways to tailor the optoelectronic response require modifying the atomic species or stoichiometry (e.g., by molecular beam epitaxy),^[1,2] quantum confinement,^[13,14] or induced lattice strain.^[15–18]

Semiconductor materials can absorb photons with energies above the bandgap energy to generate free charge carriers. Some of these carriers recombine, resulting in photoluminescent emission that can be repeatedly absorbed and re-emitted, a process called photon recycling. This process causes an intense internal photon gas to build up within the semiconductor, which leads to a large free carrier density at open-circuit conditions that

has enabled record efficiency GaAs solar cells,^[19,20] as well as the high open-circuit voltages in perovskite materials.^[21–23] One pathway to increase the internal photon density is by restricting the luminescent emission angles, which can be accomplished with the addition of a reflective dome,^[24] a multilayer stack,^[25] photonic crystals,^[26,27] or by surrounding the semiconductor with an epsilon-near-zero material.^[28–30] However, to date, all photon recycling approaches are based on passive strategies. If one could modulate, in real time, the internal photon density of semiconductors, which would allow for the active control of the device's dark current, it would enable low-power current switches and transistors with unprecedented performance without changing the underlying material.


Here, we introduce and experimentally demonstrate the concept of actively controlled photon recycling to modulate materials' optoelectronic response without altering the underlying semiconductor. We first use a spectrally selective reflector to show that energy from the internal photon gas can be used to shift the material's luminescence to higher energies. We apply this concept to enhance the open-circuit voltage of a GaAs solar cell through increased recycling of near-bandgap photons, without restricting its absorption or emission angles. Finally, we control the dark current in a p–n junction diode, in real-time, using a reflectivity-switching device that actively modulates the amount of photon recycling. These capabilities provide an all-photonic paradigm for tuning the optoelectronic response of a semiconductor without altering its structural properties, chemical composition, or its operation conditions (temperature, pressure, bias, etc.).

Dr. Y. Xu, E. M. Tennyson, Dr. J. Kim, S. Barik, Dr. J. Murray,
Prof. E. Waks, Prof. M. S. Leite, Prof. J. N. Munday
Institute for Research in Electronics and Applied Physics
University of Maryland
College Park, MD 20740, USA
E-mail: jnmunday@umd.edu

Dr. Y. Xu, Dr. J. Kim, Dr. J. Murray, Prof. E. Waks, Prof. J. N. Munday
Department of Electrical and Computer Engineering
University of Maryland
College Park, MD 20740, USA

E. M. Tennyson, Prof. M. S. Leite
Department of Materials Science and Engineering
College Park, MD 20740, USA

S. Barik
Department of Physics
University of Maryland
College Park, MD 20740, USA

 The ORCID identification number(s) for the author(s) of this article can be found under <https://doi.org/10.1002/adom.201701323>.

DOI: 10.1002/adom.201701323

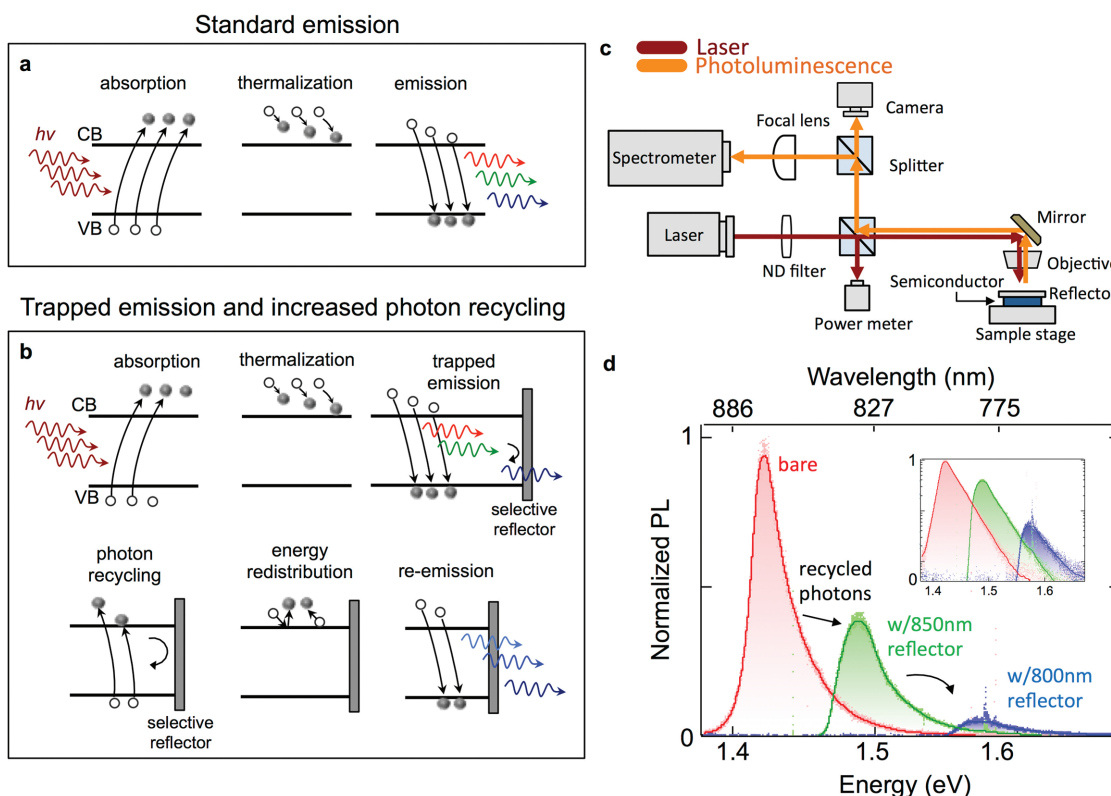


Figure 1. Increased high-energy photoluminescence (PL) through photon recycling. a) For a standard semiconductor, absorption results in carrier generation, followed by thermalization to the band-edge, and subsequent photon emission with a spectrum peaked near the semiconductor bandgap energy. b) The addition of a spectrally selective reflector causes light that would normally be emitted to be trapped and reabsorbed (increased photon recycling). The newly generated carriers exchange energy with other carriers in the conduction band, and recombination and photon emission occurs again. Only photons emitted with energy greater than the reflector's cutoff energy will escape to be detected. c) Schematic of PL experimental setup. d) PL measurements for bare GaAs and GaAs with reflector system, showing modified photon emission. The increased photon flux at higher energies is a result of energy transfer between excited carriers facilitated by photon recycling. Inset shows the PL intensity in log-scale.

Figure 1 shows how photon recycling can be used to increase the energy of emitted photons, resulting in a blue shift of the photoluminescence (PL) spectrum. A semiconductor absorbs incident light above its bandgap, generating charge carriers. These carriers quickly thermalize with each other and with the lattice (within picoseconds to nanoseconds) before finally recombining to generate photons with energy near the semiconductor bandgap (see Figure 1a for the standard photon emission process). Alternatively, when we add a coating to the top of a semiconductor to selectively reflect near-bandgap photons, the photons are instead reflected back into the material and reabsorbed, resulting in increased photon recycling (see trapped emission in Figure 1b). These reabsorbed photons generate new carriers that interact with the lattice and other carriers, causing a redistribution of the energy before carrier recombination yields secondary photon emission. Note that only photons emitted with energy higher than the cutoff energy for the selective reflector will escape, resulting in PL emission. The photons that are not emitted are then reabsorbed and continue the recycling process until either a photon is generated with enough energy to pass through the reflector or the generated carriers recombine nonradiatively. Thus, when nonradiative recombination is minimal, the intensity of the high-energy

PL is greater with the reflectors than for the bare semiconductor, which is a key signature of this phenomenon.

We confirm the photon recycling process (and the increased density of high-energy carriers) by room temperature PL measurements. The experimental setup and data are presented in Figure 1c,d, where three selective reflectors are placed on top of a GaAs wafer, which reflect photons with energy (wavelength) below (longer than) their individual cutoffs of 1.459 eV (850 nm), 1.550 eV (800 nm), and 1.653 eV (750 nm)—see the Experimental Section and Figure S2 (Supporting Information). The PL spectra are calibrated such that their relative intensities can be compared (Experimental Section). Upon the addition of the reflector with $E_{\text{cutoff}} = 1.459$ eV (850 nm), two effects occur. First, the peak of the PL signal shifts to higher energy values (from ≈ 1.42 eV for the bare GaAs (red curve) to 1.49 eV for the GaAs with reflector (green curve) in Figure 1d). Secondly, the peak intensity of the PL signal at that energy (1.49 eV) increases by more than a factor of 3 compared to the bare GaAs. Because the internal fluorescence yield η_{int} of this GaAs sample is $\approx 83\%$ (Experimental Section), repeated photon recycling has diminishing returns, limiting the effect in this case. For the reflector with $E_{\text{cutoff}} = 1.550$ eV (800 nm), there is still a substantial shift in the PL peak. Although the intensity of its peak is further

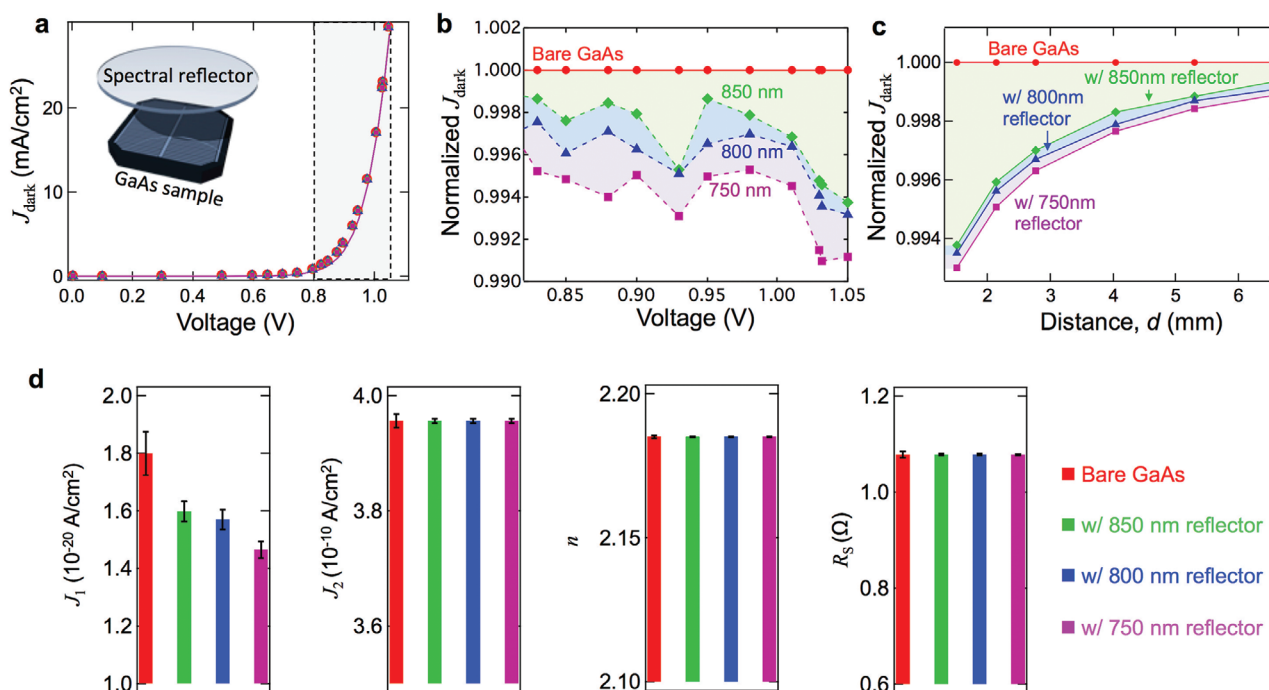


Figure 2. Dark current reduction through photon recycling. a) $J_{\text{dark}}-V$ measurements for a bare GaAs solar cell [red circles] and the same device with the addition of selective reflectors with cutoff energies (wavelengths) of 1.459 eV (850 nm) [green diamonds], 1.550 eV (800 nm) [blue triangles], and 1.653 eV (750 nm) [purple squares]; note: symbols overlap at this scale. Overlapping solid lines correspond to the fitting of the two-diode model for the GaAs device with and without the reflectors. Inset: schematic of experimental configuration. b) Ratio of the dark current densities for devices with reflectors to that without, corresponding to the shaded region in (a). c) Normalized dark current density as a function of the distance, d , between the GaAs solar cell and the reflectors [see schematic in (a)], showing how the effect is more pronounced as the vertical displacement of the reflectors is reduced. d) Histograms of relevant device parameters measured with and without selective reflectors. While most parameters remain unchanged upon the addition of the reflectors, the dark current density J_1 , related to carriers' radiative recombination, is reduced. The error bars refer to three standard deviations of the data from the mean value.

reduced, the PL signal near 1.55 eV is higher with this reflector than for the other cases (see Figure inset). Ultimately, the reflectors substantially enhance the internal photon density by recycling the light emitted with energies between the cutoff and the original bandgap of GaAs (i.e., for all emitted photons that can be reflected back into the material). These photons act as a secondary source of illumination, which creates additional carriers within the semiconductor. Thus, the optoelectronic response of semiconductor devices could potentially be engineered through photonic means without changing the chemical composition or the crystalline lattice of the material.

In addition to the modified optical response, the semiconductor's electronic properties also change by incorporating the reflectors, even without illumination. The current density-voltage ($J-V$) characteristic for a simple p-n junction in the dark (J_{dark}) can be described by a two-diode model as^[31]

$$J_{\text{dark}}(V) = J_1 \left(e^{\frac{q[V - J_{\text{dark}}(V)R_s]}{k_B T}} - 1 \right) + J_2 \left(e^{\frac{q[V - J_{\text{dark}}(V)R_s]}{nk_B T}} - 1 \right) + \frac{V - J_{\text{dark}}(V)R_s}{R_{\text{shunt}}}, \quad (1)$$

where V is the applied voltage, J_1 and J_2 are the dark current density components corresponding to diode ideality factors of one (primarily due to radiative recombination in a high-quality

device) and n (which is ≈ 2 and is mostly due to nonradiative recombination within the junction under low-level injection), respectively, k_B is the Boltzmann constant, T is the device temperature ($\approx 25^\circ\text{C}$), q is the electron charge, R_s is the series resistance, and R_{shunt} is the shunt resistance of the device. The addition of a photon reflector to the top of the device reduces J_1 , increasing the applied voltage necessary to reach a particular current value.

We experimentally determine the effect of the spectrally selective reflectors on the electronic response of a GaAs p-n junction device by measuring its dark current characteristics with and without the reflectors, as shown in Figure 2. The dark current measurements are fit to the two-diode model (Equation (1)) in the high-voltage region (from 0.6 to 1.05 V), where radiative emission is the primary component. The model represents the experimental data very well, with J_1 , J_2 , n , and R_s as fit parameters (Figure 2a,b). Further, the reduction in the dark current is most significant for reflectors with a higher energy (lower wavelength) cutoff, corresponding to an increase in the number of recycled photons. The $J-V$ characteristics are used to determine the diode parameters for the device with and without the different reflectors. The dark-current density component corresponding to radiative recombination (J_1) is clearly reduced with the addition of the reflectors (see Figure 2d), as desired. The other parameters, J_2 , n , and R_s , remain unchanged. As the distance between the reflector and the device

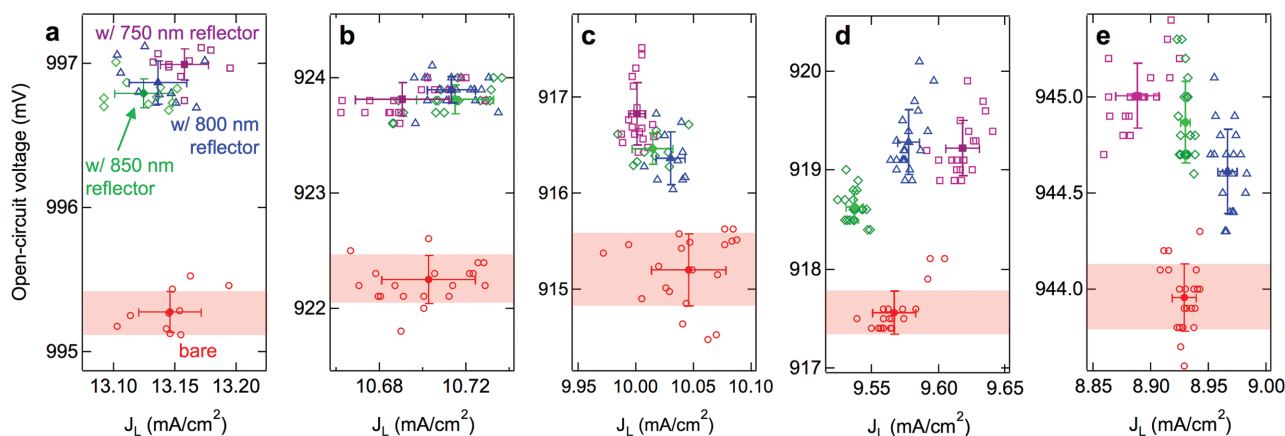


Figure 3. Open-circuit voltage enhancement in a GaAs solar cell. Open-circuit voltage, V_{oc} , under AM1.5G spectrum (0.6 suns illumination) for a GaAs solar cell without [bare GaAs, red] and with selective reflectors with cutoff energies (wavelengths) of 1.459 eV (850 nm) [green], 1.550 eV (800 nm) [blue], and 1.653 eV (750 nm) [purple]. a) For similar short-circuit current densities, the V_{oc} is increased by 1.51 ± 0.25 , 1.59 ± 0.30 , and 1.71 ± 0.24 mV, respectively. The error bars represent the standard deviation of the measured mean value. b–e) Measurements performed on four additional days under slightly different illumination conditions all show similar behavior.

is increased, the photon recycling is continuously reduced as more photons can now escape the semiconductor, see Figure 2c. When the spacing between the reflector and the GaAs diode approaches 1 cm, the effect of the reflector is diminished, and the dark current for all devices converges to the same value.

By increasing the internal photon density, we also improve the voltage response of solar cells without limiting their acceptance angle for incident light. We analyze the changes in the open-circuit voltage (V_{oc}) caused by the addition of selective reflectors based on current–voltage measurements (Experimental Section and Figure S3, Supporting Information). For an ideal solar cell, the V_{oc} is given by

$$V_{oc} = \frac{k_B T}{q} \ln \left(\frac{J_L}{J_{dark}} + 1 \right) \quad (2)$$

where J_L is the light-generated current density. If the dark current density near V_{oc} is dominated by radiative emission, which is the case for high-quality direct bandgap semiconductors, J_{dark} can be suppressed by using the spectrally selective reflectors, as shown above. We keep J_L fixed (13.15 ± 0.10 mA cm⁻²) by adjusting the incident illumination from a solar simulator to ensure that any changes in V_{oc} are uniquely due to the reduction in J_{dark} and not a result of changes in J_L due to the reflector's response away from its cutoff energy (which could potentially modify J_L). After applying the three energy selective reflectors, the V_{oc} increases by 1.51 ± 0.25 , 1.59 ± 0.30 , and 1.71 ± 0.24 mV, respectively, for cutoff energies of 1.459 eV (850 nm), 1.550 eV (800 nm), and 1.653 eV (750 nm), as shown in Figure 3a. Because the voltage enhancement comes from the decrease in J_{dark} , reflectors with higher energy cutoffs enable a larger V_{oc} . We perform each J – V measurement set at least 40 times on distinct days to exclude the influence of thermal variations in the ambient and of differences in the electrical contacts, as summarized in Figure 3. We also vary the illumination conditions (≈ 0.6 suns using the AM1.5G spectrum) slightly to show the robustness of the measurements. In all cases, the V_{oc} is enhanced by 1–2 mV with the addition of the reflectors. We

use a standard glass slide as a control, confirming no change in V_{oc} upon its addition. For higher illumination intensities (e.g., using optical concentration), we expect further increases in the V_{oc} when the reflectors are used so long as the device operation remains in the low injection regime.

As a key demonstration of our approach, we construct a current switch that operates by actively controlling the photon emission recycling. The structure consists of a GaAs p–n junction diode with a reflectivity-control component (Figure 4) formed by a polymer-dispersed liquid crystal with a silver mirror.^[32] The reflectivity-control component has two states. When a voltage is applied (ON state, see Figure 4a,c), the liquid crystal droplets align. Light passes through the layer, exposing the silver mirror, which causes this component to have mirror-like reflectivity. In the OFF state (no applied bias, see Figure 4b,d), the liquid crystal droplets are randomly oriented, and light is scattered in all directions (acting as a diffuser). In the OFF state, the total reflectivity is reduced, and thus fewer photons are reflected back into the GaAs for photon recycling.

When the reflectivity-control component is placed on top of the GaAs diode, we can actively regulate whether the photons generated by carrier recombination in the dark are able to exit the diode (diffusive, OFF state) or are reflected back (mirror-like, ON state) for additional photon recycling. To test this effect, the diode current is recorded in the dark GaAs p–n junction reduced for a given applied bias across the diode when the reflectivity-control component is in the OFF state. For this situation, most photons emitted from the p–n junction exit the GaAs and are lost. However, in the ON state, it becomes more reflective and increases the photon recycling, which in turn reduces the dark current in the p–n junction (Figure 4e). Hence, we actively control the produced dark current. The switchability is significantly diminished if the mirror is replaced by an absorbing layer, which decreases the photon recycling in the ON state (Experimental Section and Figure S4, Supporting Information).

The optical and electrical experiments presented here independently demonstrate that photon recycling can be dynamically modulated via external stimuli, enabling a new, all-optical

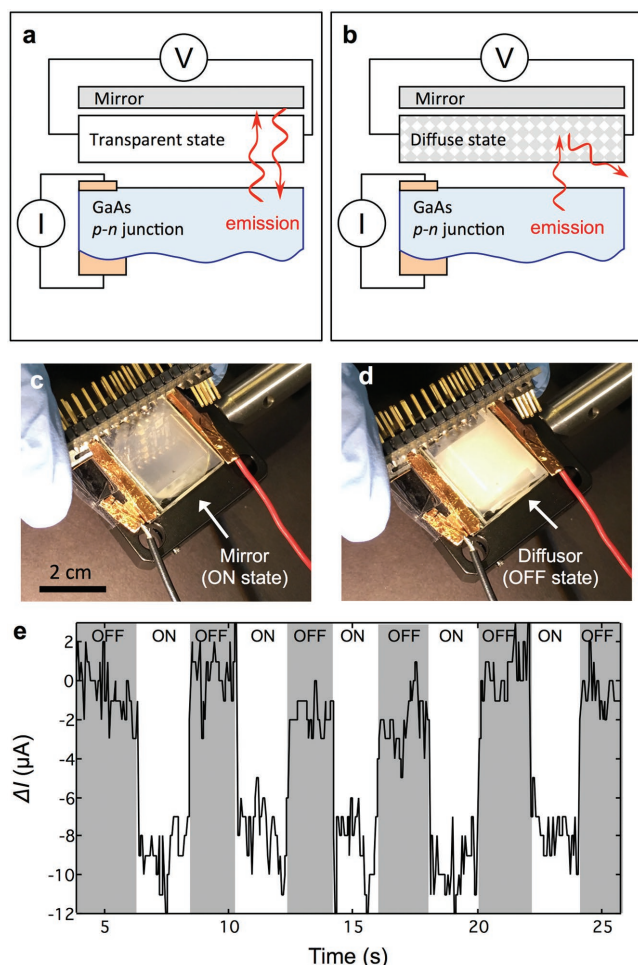


Figure 4. Current switching device based on active control of photon recycling. a,b) Schematic of device containing a p–n junction whose current (I) is modulated by active control of photon emission (out of scale for clarity). c) Reflectivity-control component in ON state produces mirror-like behavior and increases photon recycling. d) In the OFF state, the component acts as a diffuser and reduces the photon recycling. e) The current produced by the p–n junction is modulated (ΔI) as the reflectivity-control component changes state through the application of an applied voltage (V).

approach to tailoring the optoelectronic response of a single semiconductor in real time. This behavior is used to modify the semiconductor emission wavelengths, as well as modulate the device's dark current. Larger effects can be achieved using semiconductors with higher internal fluorescence yield and by using higher quality spectral reflectors. While the currently implemented reflectors are able to reflect >95% of the emitted photons, the refractive index contrast between the air and the semiconductor decreases the amount of emission that is reabsorbed due to the impedance contrast for photons re-entering the semiconductor. For instance, an ideal reflector with a cut-off wavelength of 750 nm and perfect recoupling into the GaAs solar cell (e.g., by directly depositing the reflector onto the GaAs) would yield a ≈ 166.7 mV improvement of the V_{oc} for a photovoltaic device with an internal fluorescence yield of 99.7%, which has been reported for the highest quality III-V materials.^[33]

In conclusion, we have shown how controlled photon emission recycling modifies a semiconductor's optoelectronic response through an all-photon approach without changing the material composition or structure. To demonstrate this concept, we measured a shift in the optical (emission spectrum) and electrical (dark current) responses of various GaAs devices. The emission recycling process increased the V_{oc} of a solar cell by reducing its dark current. Further, we demonstrated a gate-free, current switch based on actively tunable photon recycling. Our approach will likely find practical applications ranging from photodetectors to actively controlled current switches. While we have used GaAs for the above demonstrations, these principles hold for any material with a high internal fluorescence yield (e.g., InP, perovskites, etc.). For photovoltaics, this phenomenon can be used as a method to tailor the absorption and emission properties of a semiconductor material to more closely match the incident solar spectrum. Specifically, for low bandgap semiconductors that produce high current but low voltage, the addition of spectrally selective reflectors could be implemented to match the ideal current-voltage characteristic.^[34] Additionally, spectrum splitting photovoltaic designs could be improved using reflective optical components rather than requiring new material growth. Photodetectors could be designed with reduced dark current to increase the signal-to-noise ratio, lasers could have reduced lasing thresholds,^[35] and wide bandgap semiconductors used for power electronics could achieve switching at larger voltages. We anticipate that the concept presented here will likely influence the design of the next generation of optoelectronic devices by enabling new material and device functionality from a single semiconductor.

Experimental Section

Absorption Measurements: Light absorption was measured using a 6 inch integrating sphere (Labsphere) and a xenon light source (Thermo Oriel). The white light was separated into different wavelengths by a SPEX 500M monochromator, which was passed through a chopper wheel for lock-in detection (SR830). Parasitic absorption near the band-edge due to trap states was removed using the photoluminescence signal.^[36]

GaAs Solar Cell: GaAs solar cells (Millennium Communication Co., Ltd.) were epitaxially grown on a 300 μm thick n-type GaAs wafer, and the active regions were cladded by AlGaAs passivation and back surface field layers (see Figure S1, Supporting Information).

Photoluminescence Measurements: Photoluminescence (PL) measurements were conducted using a 660 nm wavelength diode laser to excite carriers within the GaAs. The PL signal was collected through an objective (100 \times magnification, NA = 0.7), which was subsequently sent to a CCD camera and spectrometer for detection. The intensity of the PL is proportional to the carrier density,^[37] and thus its relative intensity was used to determine its change. Because the addition of a selective reflector slightly modified both the incident light beam (power density and illumination area) entering the sample and the light detected (total emission intensity), the PL signal was calibrated taking these quantities into account. The measured PL intensity is $\phi_{\text{measured}} = C \phi_{\text{PL}}(\rho) A$, where ϕ_{PL} is the PL intensity per unit area exiting the sample upon illumination with an incident power density ρ , A is the area of illumination, and C is the proportionality constant that depends upon the optical path. For a given sample and reflector, A was measured using a high-resolution Hamamatsu CCD camera, and the proportionality constant C was determined by measuring the PL intensity under different illumination power densities ρ . The PL signal ϕ_{PL} was then compared between all samples.

Determination of Internal Fluorescence Yield: The internal fluorescence yield (IFY) of the GaAs was determined by two methods (one optical and one electrical). First, IFY was directly measured through a PL experiment. The incident photon flux from a laser beam was measured and the absorption within the GaAs was determined from the reflection and transmission. The emitted photon flux was used to determine the internal fluorescence intensity, which was reduced from its theoretical maximum value due to nonradiative recombination, yielding $\eta_{\text{int}} = 83 \pm 3\%$ by this method. Secondly, the IFY was determined from the dark current measurements. For this method, the J_1 term in Equation (1) gives the externally emitted photon flux at open-circuit conditions. In the limit of small series resistance, the IFY is approximately given by^[34,38]

$$\eta_{\text{int}} = \frac{4n_{\text{sc}}^2 J_1 \exp\left(\frac{qV_{\text{oc}}}{k_B T}\right)}{4n_{\text{sc}}^2 J_1 \exp\left(\frac{qV_{\text{oc}}}{k_B T}\right) + J_2 \exp\left(\frac{qV_{\text{oc}}}{nk_B T}\right)} \quad (3)$$

where n_{sc} is the refractive index of GaAs and V_{oc} is the open-circuit voltage under 1-sun illumination, yielding $\eta_{\text{int}} \approx 83.5\%$.

Characterization of Frequency-Dependent Spectral Reflectors: The reflectors need to have a high transmission for photon energies above the selective cutoff energy and a high reflectivity for low-energy photons. Concurrently, the absorption should be as small as possible, which is measured using an integrating sphere setup, as described above. Three spectrally selective reflectors (Thorlabs dielectric shortpass filters) were used with cutoff energies (wavelengths) of 1.459 eV (850 nm), 1.550 eV (800 nm), and 1.653 eV (750 nm). The absorption within each reflector was measured to be <5% within the wavelength of interest (see Figure S2a, Supporting Information). The angularly dependent transmission properties of each reflector were measured using a goniometer, and a tunable laser as the illumination source. The reflectors were mounted onto a rotation stage, and the transmission spectra were acquired for an angular range between 0 and 65°, as shown in Figure S2b–d (Supporting Information). In all cases, very high transmissivity (reflectivity) was obtained above (below) the cutoff energy, as desired.

Current–Voltage Measurements of GaAs Devices: Current–voltage measurements were performed using a Keithley 2420 Source Meter, and a Newport Model 91159 Full Spectrum Solar Simulator was used for illuminated measurements.

Current–Voltage Characteristics of GaAs Solar Cells under Illumination with and without Spectral Reflectors: The I – V characteristics of the GaAs solar cell plus different selective reflectors were measured to determine the resulting change in the open-circuit voltage, as shown in Figure 3 of the main text. During each set of measurements, the incident power of the illumination source on the solar simulator was adjusted to maintain the same short-circuit current for all configurations (with and without reflectors). This ensured that any changes in voltage were uniquely due to photon recycling effects and not because of higher illumination intensity (which could also increase the density of carriers within the semiconductor). The samples were measured over multiple days, as shown by the data sets in Figure 3 of the main text to ensure the reproducibility and robustness of the results. Figure S3 (Supporting Information) shows the J – V characteristics for the bare solar cell and with three different reflectors with cutoff energies of 1.459 eV (850 nm), 1.550 eV (800 nm), and 1.653 eV (750 nm).

Current-Switching Device Based on Active Control of Photon Recycling: Two sets of experiments were performed with an actively controlled current-switch device, formed by a GaAs p–n junction and a reflectivity-control component. The first one incorporated a silver mirror and resulted in a device that changed from diffusely reflective (OFF state) to specularly reflective (ON state). The second configuration replaced the mirror with a black absorber that resulted in a device that changed between diffusely reflective (OFF state) and absorptive (ON state). In the OFF state, both devices appeared white and scattered light. In the ON state, the device with the mirror became a better reflector of photons

emitted from the GaAs, and the current in the GaAs p–n junction reduced for a given applied bias. Alternatively, the device with the absorber became a worse reflector in the ON state, and the dark current in the GaAs increased, see Figure S4 (Supporting Information).

Supporting Information

Supporting Information is available from the Wiley Online Library or from the author.

Acknowledgements

The authors acknowledge financial support by the National Science Foundation under Grant CBET-1335857. Y.X. fabricated samples and performed experiments. Y.X., E.M.T., J.K., and S.B. performed PL measurements and analysis. J.M. assisted in absorption measurements and fabrication of polymer dispersed liquid crystal devices. Y.X., J.N.M., M.S.L., and E.W. analyzed the data and wrote the manuscript. J.N.M. conceived and supervised the project. All authors reviewed the manuscript.

Conflict of Interest

The authors declare no conflict of interest.

Keywords

bandgap, light emitting diodes, optoelectronics, photon recycling, solar cells

Received: December 6, 2017
Revised: December 22, 2017
Published online: January 25, 2018

- [1] A. Y. Cho, J. R. Arthur, *Prog. Solid State Chem.* **1975**, *10*, 157.
- [2] F. Capasso, *Science* **1987**, *235*, 172.
- [3] P. Hosseini, C. D. Wright, H. Bhaskaran, *Nature* **2014**, *511*, 206.
- [4] J. A. Rogers, M. G. Lagally, R. G. Nuzzo, *Nature* **2011**, *477*, 45.
- [5] C. Euaruksakul, Z. W. Li, F. Zheng, F. J. Himpfel, C. S. Ritz, B. Tanto, D. E. Savage, X. S. Liu, M. G. Lagally, *Phys. Rev. Lett.* **2008**, *101*, 147403.
- [6] S. Wirths, R. Geiger, N. von den Driesch, G. Mussler, T. Stoica, S. Mantl, Z. Ikonik, M. Luysberg, S. Chiussi, J. M. Hartmann, H. Sigg, J. Faist, D. Buca, D. Grützmacher, *Nat. Photonics* **2015**, *9*, 88.
- [7] S. M. Sze, *Physics of Semiconductor Devices*, Wiley-InterScience, Hoboken, NY **1981**.
- [8] N. W. Ashcroft, N. D. Mermin, *Solid State Physics*, Saunders, Philadelphia **1976**.
- [9] Z. I. Alferov, *Rev. Mod. Phys.* **2001**, *73*, 767.
- [10] H. Kroemer, *Proc. IEEE* **1963**, *51*, 1782.
- [11] R. R. King, *Nat. Photonics* **2008**, *2*, 284.
- [12] Y. Nanishi, *Nat. Photonics* **2014**, *8*, 884.
- [13] A. P. Alivisatos, *Science* **1996**, *271*, 933.
- [14] M. Nolan, S. O'Callaghan, G. Fagas, J. C. Greer, T. Frauenheim, *Nano Lett.* **2007**, *7*, 34.
- [15] C. P. Kuo, S. K. Vong, R. M. Cohen, G. B. Stringfellow, *J. Appl. Phys.* **1985**, *57*, 5428.
- [16] M. S. Leite, E. C. Warmann, G. M. Kimball, S. P. Burgos, D. M. Callahan, H. A. Atwater, *Adv. Mater.* **2011**, *23*, 3801.

- [17] J. R. Sánchez-Pérez, C. Boztug, F. Chen, F. F. Sudrajat, D. M. Paskiewicz, R. Jacobson, M. G. Lagally, R. Paiella, *Proc. Natl. Acad. Sci. USA* **2011**, *108*, 18893.
- [18] J. Michel, J. Liu, L. C. Kimerling, *Nat. Photonics* **2010**, *4*, 527.
- [19] O. D. Miller, E. Yablonovitch, S. R. Kurtz, *IEEE J. Photovoltaics* **2012**, *2*, 303.
- [20] V. Ganapati, M. A. Steiner, E. Yablonovitch, *IEEE J. Photovoltaics* **2016**, *6*, 801.
- [21] E. Yablonovitch, *Science* **2016**, *351*, 1401.
- [22] L. M. Pazos-Outón, M. Szumilo, R. Lamboll, J. M. Richter, M. Crespo-Quesada, M. Abdi-Jalebi, H. J. Beeson, M. Vrućinić, M. Alsari, H. J. Snaith, B. Ehrler, R. H. Friend, F. Deschler, *Science* **2016**, *351*, 1430.
- [23] Y. Fang, H. Wei, Q. Dong, J. Huang, *Nat. Commun.* **2017**, *8*, 14417.
- [24] A. Braun, E. A. Katz, D. Feuermann, B. M. Kayes, J. M. Gordon, *Energy Environ. Sci.* **2013**, *6*, 1499.
- [25] E. D. Kosten, B. M. Kayes, H. A. Atwater, *Energy Environ. Sci.* **2014**, *7*, 1907.
- [26] Y. Shen, D. Ye, I. Celanovic, S. G. Johnson, J. D. Joannopoulos, M. Soljačić, *Science* **2014**, *343*, 1499.
- [27] J. D. Joannopoulos, P. R. Villeneuve, S. Fan, *Nature* **1997**, *386*, 143.
- [28] Z. Wang, Z. Wang, Z. Yu, *Appl. Phys. Lett.* **2016**, *109*, 051101.
- [29] N. Engheta, *Science* **2013**, *340*, 286.
- [30] I. Liberal, N. Engheta, *Nat. Photonics* **2017**, *11*, 149.
- [31] M. Wolf, G. T. Noel, R. J. Stirn, *IEEE Trans. Electron Devices* **1977**, *24*, 419.
- [32] J. Murray, D. Ma, J. N. Munday, *ACS Photonics* **2017**, *4*, 1.
- [33] I. Schnitzer, E. Yablonovitch, C. Caneau, T. J. Gmitter, A. Scherer, *Appl. Phys. Lett.* **1993**, *63*, 2174.
- [34] J. N. Munday, *J. Appl. Phys.* **2012**, *112*, 064501.
- [35] F. Stern, J. M. Woodall, *J. Appl. Phys.* **1974**, *45*, 3904.
- [36] T. Trupke, E. Daub, P. Würfel, *Sol. Energy Mater. Sol. Cells* **1998**, *53*, 103.
- [37] T. Trupke, R. A. Bardos, M. D. Abbott, J. E. Cotter, *Appl. Phys. Lett.* **2005**, *87*, 093503.
- [38] Y. Xu, J. N. Munday, *IEEE J. Photovoltaics* **2014**, *4*, 233.